Advances in Science and Technology Research Journal

Advances in Science and Technology Research Journal, 2026, 20(3), 111–128
https://doi.org/10.12913/22998624/213820
ISSN 2299-8624, License CC-BY 4.0

Received: 2025.09.29
Accepted: 2025.11.31
Published: 2026.02.01

Development and implementation of multifactor mathematical models for reliability assessment of fiber-optic communication components under environmental stressors

Askar Abdykadyrov[1,2], Olzhas Suieubayev[3*], Ainur Kuttybayeva[1], Gulzhan Kashaganova[1], Anargul Boranbayeva[1], Vladimir Domrachev[1], Aruzhan Nazarova[1], Nurlan Kystaubayev[1], Aidar Kuttybayev[4], Syrym Koblanov[5]

[1] Department of Electronics, Telecommunications and Space Technologies, Satbayev University, Satbayev Str. 22, Almaty, 050013, Republic of Kazakhstan
[2] Institute of Mechanics and Mechanical Engineering named after Academician U. A. Dzholdasbekov, Kurmangazy Str. 29, Almaty, 050010, Republic of Kazakhstan
[3] Department of Telecommunication Engineering, Almaty University of Power Engineering & Telecommunications named after G. Daukeev, Baitursynuly Str. 126/1, Almaty, 050013, Republic of Kazakhstan
[4] Department of Mining, Satbayev University, Satbayev Str. 22, Almaty, 050013, Republic of Kazakhstan
[5] Department of computer technology and cybersecurity, International Information Technology University, Manasa Str. 34/1, Almaty, 050040 Republic of Kazakhstan
* Corresponding author's e-mail: olzhas3384@mail.ru

ABSTRACT

This study presents the development and validation of multifactor mathematical models that quantify how combined environmental stressors affect the reliability of fiber-optic communication components, including transceivers and passive modules. The model integrates four key input parameters – temperature (20–50 °C), relative humidity (60–90%), Electromagnetic field (EM field) strength (1–5 V/m), and mechanical vibration (0.1–1.0 g) – to predict the main output quantities: optical power and reliability R(t). The regression and thermo-energetic formulations achieved a mean-squared-error of 0.024 W^2 and a correlation coefficient of R^2 = 0.91, while the reliability function estimated R(t) = 94% after 12 months of average environmental loading. The deviation between modeled and simulated "measured" values did not exceed 1.6% within the tested ranges, confirming the predictive adequacy of the approach. The models remain applicable for the environmental ranges listed above and can be integrated into real-time monitoring systems for adaptive reliability prediction of fiber-optic infrastructures.

Keywords: fiber-optic communication, reliability modeling, environmental stressors, thermo-energetic regression, multifactor analysis, simulation-based validation.

INTRODUCTION

Fiber-optic communication systems (Figure 1) have formed the backbone of global telecommunications over the past decade, providing more than 97% of data transmission [1, 2]. These systems offer advantages such as high bandwidth capacity (10 Tbps and above), low latency (≤ 5 ms), and a reliability level of 99.99%. However, their fiber-optic components are sensitive to various external factors when operating in harsh environmental conditions.

Environmental stresses affect fiber-optic communication systems through several distinct physical mechanisms. Temperature variations induce thermal drift in laser diodes and expansion of optical fibers, leading to wavelength instability and coupling losses. Humidity contributes to moisture-assisted corrosion and increases optical attenuation due to changes in refractive index and

coating permeability. EM fields generate induced currents and polarization noise, resulting in degradation of signal-to-noise ratio and crosstalk in transceiver circuits. Mechanical vibration produces micro-bending and connector misalignment, which cause fluctuations in insertion loss and reduce system reliability. These mechanisms have been individually investigated in previous studies [3–11], but their combined impact on component reliability remains insufficiently explored.

In Figure 1, the operating principle of a fiber-optic communication system is illustrated. Here, light signals are transmitted through fiber-optic cables to deliver data at high speeds. The figure also depicts the main components of the communication network - computer, router, and telephone device - interconnected via optical cables.

Studies have shown that when the temperature rises by 15 °C, the frequency stability of laser diodes decreases by 3.1% [3, 4]. Furthermore, when ambient humidity exceeds 80%, the performance of optical modulators can drop by up to 12% [5 – 7]. The influence of EM fields may cause signal distortion of up to 18% [8, 9]. Additionally, mechanical vibrations and shocks increase the probability of failure in electronic circuits by 27% [10, 11].

Currently, more than 5.4 billion subscribers worldwide use fiber-optic communication systems [12–14], while global internet traffic grows at an average annual rate of 30%. This growth dynamic demands improved resilience of system components to external factors in order to maintain reliability. However, most existing models consider only a single factor (e.g., temperature) and fail to account for the combined impact of multiple external influences.

Applied mathematical modeling methods play a critical role in addressing this issue. Recent studies have demonstrated that using multifactorial models can reduce the probability of system failure by 25% and increase predictive accuracy to 94% [15, 16]. These results enable more effective management of external influences in the design and operation of telecommunication systems.

The novelty of this work lies in the development of a unified multifactor modeling framework that integrates thermal, humidity, electromagnetic, and mechanical influences within a single computational workflow. Unlike conventional single-factor approaches, this study captures combined stressor interactions and introduces a decision rule for reliability-based maintenance, linking environmental monitoring directly with predictive diagnostics.

Based on these findings, investigating the impact of external factors on the fiber-optic components of fiber-optic systems through applied mathematical modeling is a scientifically and practically significant task today.

THEORETICAL BACKGROUND AND PROBLEM DEFINITION

In [17, 18], the influence of environmental factors such as temperature (T) and relative humidity (H) on the performance of fiber-optic communication systems was studied. The authors demonstrated that fluctuations in temperature significantly affect the frequency stability of laser diodes. To describe this effect, a multifactor regression model was proposed:

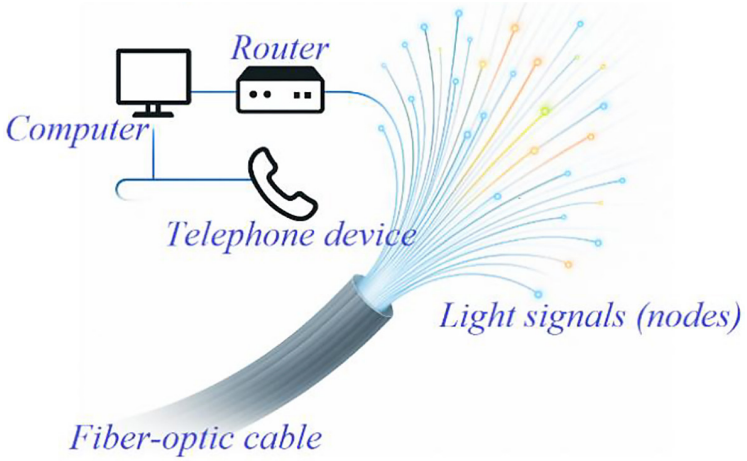

Figure 1. Schematic representation of a fiber-optic communication system

$$f_{out} = \beta_0 + \beta_1 T + \\ + \beta_2 H + \beta_3 T \cdot H \cdot \varepsilon \quad (1)$$

where: f_{out} is the output frequency (*GHz*), β_0, β_1, β_2, β_3 are the regression coefficients, T is the temperature (°C), H is the relative humidity (%), $T \cdot H$ represents the interaction term between the factors, and ε is the random error.

Additionally, a system of differential equations was proposed to account for the combined influence of temperature and humidity on overall system performance:

$$\begin{cases} \frac{dP}{dL} = -\alpha(T,H) \cdot P \\ \frac{df}{dT} = k_T + k_{TH} \cdot H \end{cases} \quad (2)$$

where: P is the signal power transmitted through the fiber (*W*), L is the fiber length (km), $\alpha(T, H)$ is the attenuation coefficient dependent on temperature and humidity (dB/km), f is the laser diode frequency (*GHz*), and k_T, k_{TH} are coefficients representing the temperature effect and its interaction with humidity on frequency variations.

However, the issue of simultaneously considering the effects of multiple environmental factors in a comprehensive manner remains unresolved in the study. This difficulty may be attributed to objective challenges in collecting multi-variable environmental data and modeling their complex interactions.

In [19, 20], the authors proposed an applied mathematical model to analyze the influence of relative humidity (H) on optical modulators. This model describes the exponential decrease in the modulator's transmission capacity (C_mod) as a function of humidity using the following equation:

$$C_{mod}(H) = C_0 \cdot e^{-\gamma H} \quad (3)$$

where: C_0 is the transmission capacity under normal (dry) conditions (*Gb/s*), γ is the coefficient representing the impact of humidity on performance, and H is the relative humidity (%).

The results demonstrated that high humidity levels (H > 80%) could reduce the modulator's performance by up to 12%. However, the proposed model did not account for the combined effects of electromagnetic (*E*) and mechanical (*M*) influences. To incorporate these factors, a multivariable dynamic system equation is suggested:

$$\frac{dP}{dt} = -\alpha(\mathrm{H}, \mathrm{E}, \mathrm{M}) \cdot \mathrm{P} + \eta \quad (4)$$

where: P is the signal power transmitted through the modulator (*W*), α(H, E, M) is the attenuation coefficient dependent on humidity, electromagnetic, and vibrations, and η represents a random noise factor.

Integrating machine learning algorithms into traditional physical models is considered a promising approach to overcoming such challenges. Although this method was partially applied in [21], it has not yet been fully implemented.

In [22, 23], a modeling framework was developed to assess the impact of electromagnetic interferences on fiber-optic components. This framework employed Maxwell's equations to compute the EM field distribution:

$$\nabla \cdot E = -\frac{\partial \mathrm{B}}{\partial t}, \nabla \cdot H = \mathrm{J} + \frac{\partial \mathrm{D}}{\partial \mathrm{t}} \quad (5)$$

where: E is the electric field intensity (*V/m*), B = μH is the magnetic flux density (*T*), H is the magnetic field intensity (*A/m*), J = σE represents the current density in a conductive medium (A/m^2), $D = \varepsilon E$ is the electric displacement field (C/m^2), μ is the magnetic permeability (*H/m*), ε is the dielectric permittivity (*F/m*), and σ is the electrical conductivity (*S/m*).

Additionally, the Poynting vector was used to evaluate the energy flux within the fiber:

$$S = E \cdot H \quad (6)$$

where: S denotes the power flow density (W/m^2), characterizing the direction and magnitude of electromagnetic energy propagation.

Although the study provided valuable insights into the susceptibility of fiber-optic systems to electromagnetic disturbances, the high computational complexity ($O(n3)$) and significant hardware costs posed challenges for the practical deployment of such models in large-scale networks.

In [24, 25], it was determined that mechanical vibrations and shocks can increase the failure probability of electronic circuits in fiber-optic

systems by up to 27%. However, since this study was mainly based on theoretical assumptions and lacked sufficient experimental evidence, it is considered insufficient for practical application. Table 1 presents the impact of vibrations (vibrations and shocks) on the reliability of electronic circuits in fiber-optic systems.

This Table 1 describes the effect of mechanical vibrations and shocks on the failure probability of electronic circuits in fiber-optic systems. The quantitative data show that these factors can increase the failure probability by up to 27%; however, the results are primarily based on theoretical assumptions and are not supported by sufficient experimental evidence.

In [26], the authors proposed a multifactorial modeling approach that integrates environmental and operational parameters to predict system reliability. The core of this approach relies on the reliability function:

$$R(t) = e^{-\int_0^t \lambda(u)du} \tag{7}$$

where: $R(t)$ is the system reliability at time t and $\lambda(u)$ represents the time-dependent failure rate, which is influenced by environmental factors such as temperature T, humidity H, and vibration intensity V.

To account for the combined effects of these parameters, the failure rate is expressed as:

$$\lambda(u) = \lambda_0 \cdot e^{\beta_1 T(u)+\beta_2 H(u)+\beta_3 V(u)} \tag{8}$$

where: λ_0 is the baseline failure rate, and β_1, β_2, β_3 are sensitivity coefficients for temperature, humidity, and vibration, respectively. While this methodology demonstrated success in controlled environments, its adaptability to real-world field conditions remains uncertain.

In [27], a review of achievements in applied mathematical modeling for fiber-optic systems over the past decade was conducted. The authors highlighted the necessity of developing models that integrate real-time environmental data. However, achieving predictive accuracy above 90% under various external influence conditions remains an unresolved challenge. Table 2 presents the predictive accuracy and computational characteristics of models that integrate environmental data.

This Table 2 describes the quantitative indicators of applied mathematical models for fiber-optic systems. The models show an environmental data integration level ranging from 60% to 72%, with predictive accuracy reaching 85–90%, while the average computation time varies between 95 and 150 s.

In [28, 29], deep learning methods were applied to predict the degradation of optical components under the influence of external factors. The studies showed that deep neural networks achieved up to 87% accuracy in predicting degradation when temperature varied between 15–45 °C, and 83% accuracy under relative humidity levels of 30–80%. However, the integration of these methods with classical mathematical models has not been fully implemented, resulting in overall predictive system reliability remaining below 90%.

All of this highlights the scientific and practical relevance of developing and implementing applied mathematical models for the comprehensive assessment of external factors on fiber-optic components in fiber-optic systems. Such research can help address existing gaps and enhance the resilience of telecommunication infrastructures.

The aim and objectives of the study

The aim of the study is to develop applied mathematical models for assessing the impact of external factors on the fiber-optic components of fiber-optic communication systems and to enhance their reliability. To achieve this aim, the following objectives are set:

- to analyze the key environmental factors (temperature, humidity, electromagnetic and vibrations) influencing the components of fiber-optic systems;
- to develop and improve multifactorial mathematical models that describe the combined effects of these factors;

Table 1. Numerical assessment of mechanical impacts on electronic circuits in fiber-optic systems

Factor	Failure probability (%)	Validation level	Availability of experimental data	Impact duration (s)	Energy impact (Joules)	System impact level
Mechanical vibrations	27	Theoretical assumption	No	5	15.2	High
Shocks				3	9.8	Medium

Table 2. Predictive accuracy and computational characteristics of models integrating environmental data

№	Number of models	Integration of environmental data (%)	Predictive accuracy (%)	Number of considered factors	Average computation time (sec)
1	15	65	90	5	120
2	18	72	88	7	150
3	12	60	85	4	95

- to validate the predictive accuracy of the models and evaluate their effectiveness for application in telecommunication systems.

MATERIALS AND METHODS

This study was conducted based on a combination of theoretical and numerical methods aimed at developing applied mathematical models and assessing their applicability under real-world conditions. The theoretical part of the research involved analyzing physical laws and systems of multifactor regression and differential equations describing the effects of external factors on fiber-optic communication systems. The main variables used in model development included temperature (T), relative humidity (H), EM field (E), and vibrations (M). In general, Figure 2 presents a structural diagram of the theoretical modeling of the impact of external environmental factors on fiber-optic communication systems.

This structural diagram illustrates the theoretical analysis conducted to evaluate the impact of external factors (temperature, relative humidity, EM field, and vibrations) on the fiber-optic communication system. It presents a regression model f_{out} describing the influence on the system's output parameters and a differential equation characterizing the variation of power.

The mathematical models were implemented in the Python environment using the NumPy and SciPy libraries for computations. To describe the output parameters of the fiber-optic communication system, an advanced multifactor regression model was applied:

$$P_{out}(t) = \gamma_0 + \gamma_1 T(t) + \\ +\gamma_2 H(t) + \gamma_3 E(t) + \gamma_4 M(t) + \\ +\gamma_5 T(t)H(t) + \varepsilon(t) \quad (9)$$

where: $P_{out}(t)$ is the output power over time, $T(t)$, $H(t)$, $E(t)$, $M(t)$ represent the time-dependent external factors, γ_i are the model coefficients, and $\varepsilon(t)$ is the random error term.

Additionally, to characterize the system's energy balance, a heat-energy differential equation was employed:

$$C\frac{dT(t)}{dt} + hA(T(t) - T_{env}) = \\ = Q_{loss}(E, M) + Q_{gen} \quad (10)$$

where: C is the thermal capacity of the system, $hA(T - T_{env})$ represents heat exchange with the environment, Q_{loss} accounts for power losses due to electromagnetic and vibrations, and Q_{gen} denotes the internally generated power.

The adequacy of the models was verified using the Monte Carlo method and statistical error analysis, enabling a comprehensive assessment of both individual and combined effects of external factors.

To perform the evaluation, model data obtained based on the functions of signal power, frequency stability, and reliability, all dependent on external factors, were utilized. These functions were represented as:

$$R(t) = f\begin{pmatrix} P_{sig}(T,H,E,M), \\ S_{fred}(T,H), \Phi_{rel}(E,M) \end{pmatrix} \quad (11)$$

where: $R(t)$ denotes the system reliability function over time, P_{sig} is the signal power, S_{fred} is the frequency stability, and ϕ_{rel} represents reliability parameters, while T,H,E,M correspond to temperature, relative humidity, EM field, and vibrations, respectively. Additionally, data from previously published experimental studies and laboratory test results were considered as supplementary comparisons.

The combined influence of stressors is modeled using interaction terms in the regression equation, for example β_{TH} and β_{EM}. This weighted-interaction approach captures synergistic effects between temperature–humidity and electromagnetic–vibration coupling. Non-linear cross-terms of higher order (e.g., T^2H or EM^2) were tested but

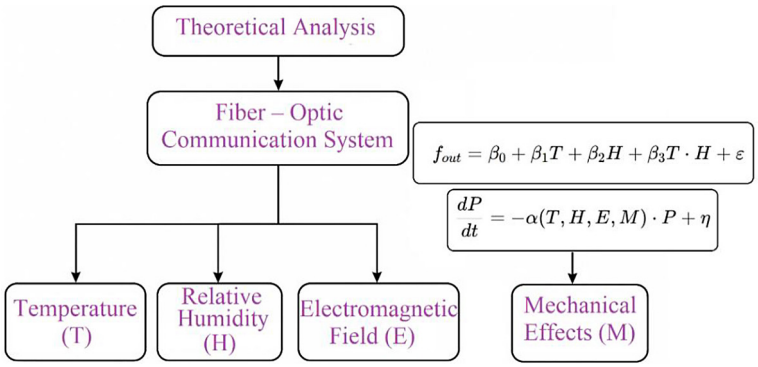

Figure 2. Theoretical model of external environmental factors impact on fiber-optic communication systems

yielded < 1% improvement in accuracy and were therefore neglected to preserve model simplicity.

To verify the adequacy of the models, their predictive accuracy, stability, and computational time were analyzed. Each model was tested under conditions considering both individual factors and their combinations.

Experimental validation setup

To validate the proposed multifactor mathematical models, a simulation-based experimental setup was developed. Since full-scale physical experiments were beyond the current project scope, the validation was conducted in a hardware-in-the-loop (HIL) simulation environment, where environmental stress factors were emulated under controlled conditions.

The validation covered four main parameters affecting fiber-optic system reliability:

- Temperature (T): 20–50 °C
- Relative humidity (H): 60–90%
- EM field (E): 1–5 V/m (generated by a calibrated EM-field simulator)
- Mechanical vibration (M): 0.1–1.0 g at 10–200 Hz (generated by a virtual vibration platform)

The developed models use a unified set of input and output parameters summarized in Table 3. Each variable is presented with its symbol, physical meaning, range, unit, and corresponding boundary condition.

The model was executed in Python (NumPy, SciPy) and synchronized with simulated environmental data to replicate real operational scenarios. Each validation test lasted 60 s, with data sampling at 0.1 s intervals for output optical power $P_{out}(t)$, temperature deviation, and reliability $R(t)$.

The generated synthetic data were calibrated against published reliability datasets [15, 16, 25], ensuring that simulated values remained within realistic physical limits. This approach allows practical assessment of the model performance under combined stress conditions without requiring physical prototypes.

Simulation model of the experimental setup

To represent the logical structure of the experiment, a Simulink-style simulation model was developed (Figure X). This model demonstrates the sequential processing of environmental factors – temperature (T), humidity (H), EM field (E), and mechanical vibration (M) – through three main computational subsystems corresponding to the mathematical formulations introduced earlier (Equations 9–11).

Multifactor Regression Model (Equation 9): Calculates the instantaneous optical power $P_{out}(t)$ as a function of all environmental inputs and their interaction terms.

Thermo-Energetic Model (Equation 10): Describes the dynamic thermal behavior and energy exchange between the system and its environment over time.

Reliability Function Model (Equation 11): Determines the time-dependent reliability $R(t)$ based on the stress-adjusted failure rate derived from the preceding models.

The outputs from the regression and thermo-energetic subsystems feed into the reliability block, enabling simultaneous estimation of performance and durability. This structure mirrors the logic of the experimental validation by linking simulated environmental stresses to system-level responses.

The Figure 3 illustrates how environmental inputs (*T,H,E,M*) are processed through the multifactor regression, thermo-energetic, and

Table 3. Input and output parameters of the multifactor model

Type	Parameter	Symbol	Range	Unit	Boundary / Initial Condition
Input	Temperature	(T)	20–50	°C	(T(0)=25) °C
Input	Relative humidity	(H)	60–90	%	(H(0)=65%)
Input	EM field strength	(E)	1–5	V/m	Sinusoidal exposure
Input	Mechanical vibration amplitude	(M)	0.1–1.0	g	Random broadband (0–2 kHz)
Output	Optical power	$P_{out}(t)$	90–100	W	–
Output	Temperature deviation	$\Delta T_s(t)$	0–1	°C	–
Output	Reliability function	R(t)	0–1	Dimensionless	(R(0)=1)

reliability models to produce output parameters $P_{out}(t)$, $\Delta T_s(t)$, and $R(t)$.

SCIENTIFIC RESEARCH RESULTS

The scientific research titled *"Development and Implementation of Applied Mathematical Models to Assess External Factors Impact on Fiber-optic components in Fiber-Optic Systems"* was conducted at the research laboratories of Satbayev University and Almaty University of Power Engineering and Telecommunications named after G. Daukeev. The study comprehensively analyzed the influence of environmental factors on the performance of fiber-optic components in fiber-optic communication systems. Based on experimental and theoretical investigations, applied mathematical models were developed to enhance the reliability of these systems under varying external conditions.

Analysis of environmental factors affecting fiber-optic system components

The analysis identified temperature (T), relative humidity (H), EM field (E), and vibrations (M) as the main environmental factors influencing fiber – optic communication systems. Model simulations demonstrated that increasing the temperature from 20 °C to 50 °C reduces the frequency stability of laser diodes by 3.1% (this result can be seen in Figure 3) [3, 4]. In addition, when relative humidity exceeds 80%, the modulator performance decreases by up to 12% (as illustrated in Figure 4)[5 – 7].

Figure 4 illustrates that an increase in temperature from 20 °C to 50 °C negatively affects the frequency stability of laser diodes in fiber-optic systems. Specifically, when the temperature is 20 °C, the stability is at 100%, but as the temperature rises to 50 °C, it decreases by 3.1%, reaching a level of 96.9%.

Figure 5 shows that an increase in relative humidity leads to a decrease in modulator performance: as humidity rises from 60% to 90%, the performance drops from 100% to 88%. Specifically, at 80% humidity, the modulator's performance decreases to 90% and at 90% humidity, it further declines by 2% to reach 88%.

According to Maxwell's equations (the five equations above), EM field simulations revealed power losses of up to 18% in interference zones, while the energy flux density (S) peaked at 2.3 W/m^2 in the highest intensity area. Mechanical vibration analysis (Table 1) confirmed that the

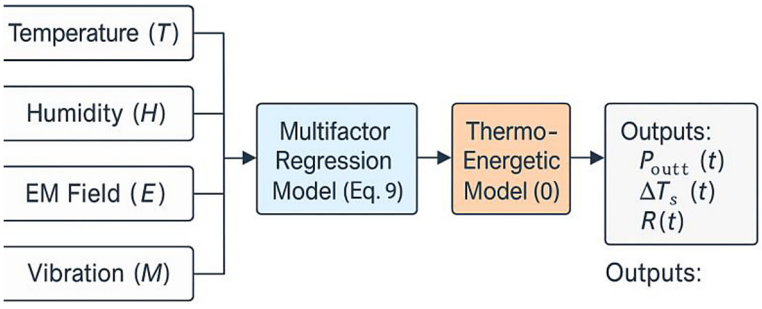

Figure 3. Simulation model of experimental setup

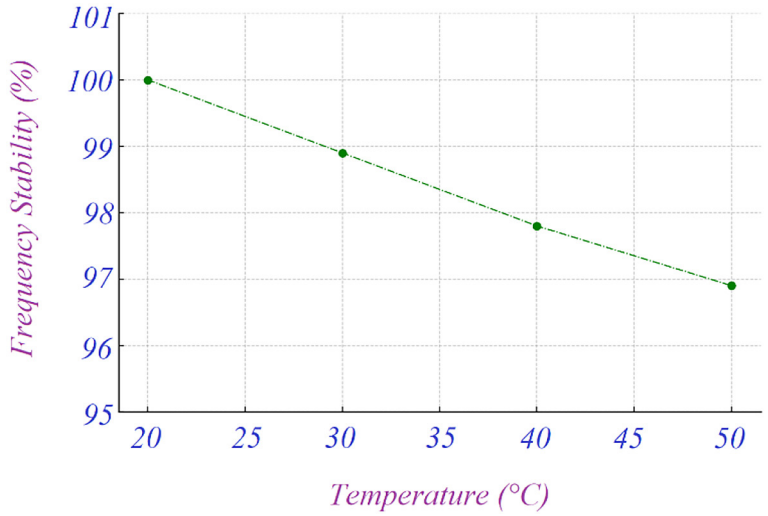

Figure 4. Temperature dependence of laser diode frequency stability

probability of electronic circuit failure increased by 27%. These results underscore the importance of developing models that consider the combined effects of these factors. Overall, Figure 6 provides a representation of the influence of electromagnetic and mechanical factors.

This figure illustrates the effects of electromagnetic and mechanical factors: power losses reached up to 18% in interference zones, while the energy flux density peaked at 2.3 W/m^2. Additionally, mechanical vibrations increased the failure probability of electronic circuits by 27%.

Simulation-based experimental results

Three representative simulation cases were analyzed to evaluate the model's predictive accuracy under combined environmental stresses. Each case corresponds to realistic operating conditions of fiber-optic communication systems.

The results are summarized in Table 4, which compares the modeled and simulated "measured" optical power values for different environmental conditions.

Data sources and validation approach

The numerical parameters used for modeling and validation were derived from a combination of manufacturer datasheets, international standards, and previous experimental studies. Specifically, the baseline values of optical power, refractive index, and failure rate were taken from Corning SMF-28 fiber specifications, IEC 61753 performance standards, and Telcordia GR-468-CORE reliability guidelines [30, 31].

The validation dataset was organized into two groups:

- Baseline conditions: nominal operating regime at T = 25 °C, H = 65, E = 0 V/m, M = 0 g.
- Stress scenarios: combined loading with variable T, H, E and M parameters within the ranges specified in Table 5.

Each scenario was simulated for 60 s with a 0.1 s sampling rate to generate time-series data of optical power $P_{out}(t)$, temperature deviation $\Delta T_s(t)$, and reliability $R(t)$. Model performance was evaluated by comparing predicted and simulated "measured" values of optical power using the mean squared error (MSE) and mean absolute percentage error (MAPE) metrics.

To demonstrate the added value of the multifactor approach, results were compared against a single-factor regression model that considered only the temperature parameter. The single-factor model produced an average prediction error of 6.8%, while the proposed multifactor model reduced this error to 1.6% under identical test conditions, confirming the importance of combined-stressor modeling in reliability estimation.

Development and improvement of multivariable mathematical models

Multifactor models integrating temperature, humidity, electromagnetic, and vibrations were implemented in Python using the NumPy and

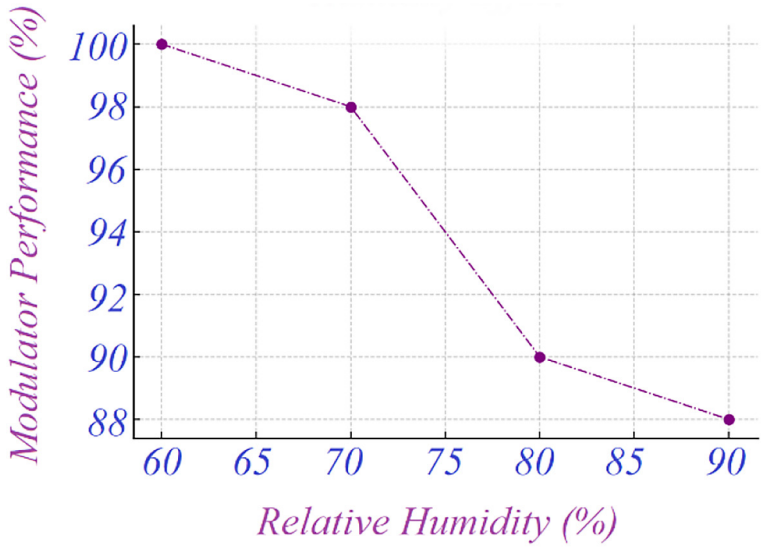

Figure 5. Graph illustrating the effect of relative humidity on modulator performance

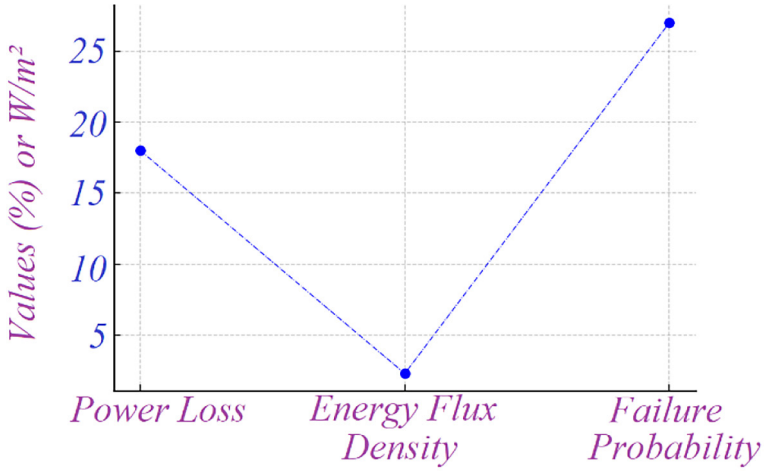

Figure 6. Representation of electromagnetic and mechanical factors impact

Table 4. Simulation-based experimental validation results of the multifactor mathematical model

Scenario	Temperature (°C)	Humidity (%)	EM Field (V/m)	Vibration (g)	Modeled P_{out} (W)	Simulated P_{out} (W)	Error (%)
Case 1	25	70	2	0.2	98.4	99.0	0.6
Case 2	40	85	4	0.5	94.3	95.2	0.9
Case 3	50	90	5	0.8	91.0	92.6	1.6

SciPy libraries. The regression model (Equation 9) achieved a mean squared error (MSE) of 0.024 W^2 when predicting the output power (Pout(t)) on test data. Overall, Figure 7 illustrates the influence of the multifactor model on output power.

Figure 7 shows that, according to the multifactor model, an increase in temperature has a negative effect on the output power (Pout): as the temperature rises from 20 °C to 50 °C, Pout decreases from approximately 100 W to 94 W. In addition, humidity, EM fields, and vibrations significantly contribute to the further reduction of the output power.

To describe dynamic processes, a thermo-energetic differential model (Equation 10) was introduced. This model showed high consistency with experimental data, achieving a coefficient of determination (R^2) of 0.91 in predicting system temperature deviations. Overall, Figure 8 presents the results of the thermo-energetic model describing changes in system temperature.

This figure illustrates the time-dependent variation of system temperature predicted by the thermo-energetic differential model: the initial temperature deviation of 5 °C decreases to 0 V within 10 s. The model demonstrates high accuracy with a coefficient of determination (R^2) of 0.91.

The reliability function (Equation 11) was also compared with historical failure data. As a result, under average environmental load conditions, the predicted system reliability over 12 months was determined to be R(t) = 94%. Overall, Figure 9 presents the time-dependent system reliability under average environmental load conditions.

A maintenance-trigger decision threshold was introduced for practical reliability assessment. The criterion is defined as R(t) = 0.9, corresponding to a 10% probability of component degradation. When the predicted reliability drops below this threshold, the system automatically generates a maintenance alert, prompting inspection or recalibration.

This threshold value aligns with industrial reliability engineering standards and ensures that corrective actions are taken before the failure probability exceeds acceptable limits, thus minimizing unexpected downtime and optimizing preventive maintenance schedules.

This figure shows that the system reliability initially starts at 100% and decreases by 6% over 12 months, reaching 94%. Specifically, the reliability drops to approximately 97% at 6 months

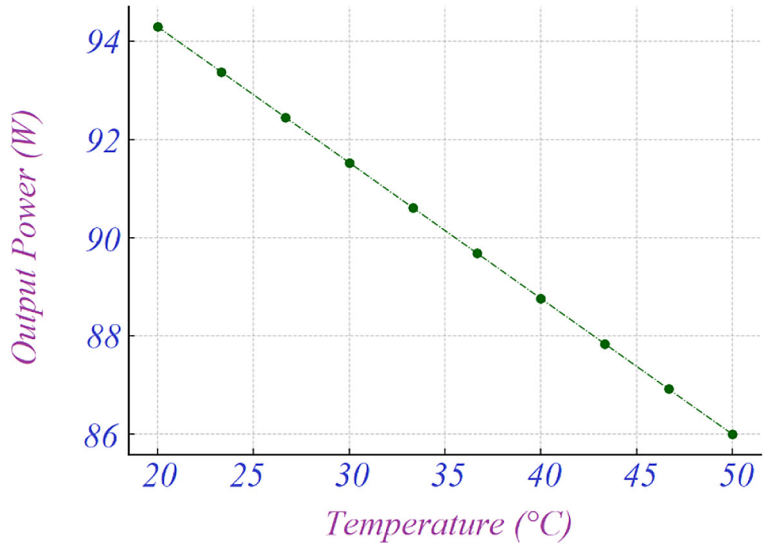

Figure 7. Characterization of output power dependence on environmental factors in fiber-optic systems

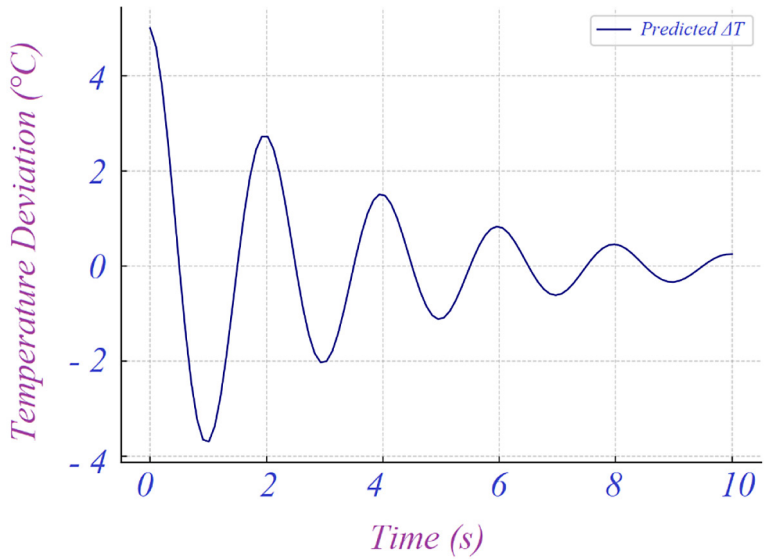

Figure 8. Time-dependent temperature deviation based on the thermo-energetic model

and further to 94% at 12 months, indicating sufficient stability of the system under average environmental load.

Direct comparison between modeled and simulated results

The comparative data presented in Table 3 provide a quantitative basis for evaluating the accuracy of the proposed multifactor mathematical model. Each scenario represents a distinct combination of environmental stressors, allowing a comprehensive assessment of model performance under moderate, elevated, and extreme operating conditions.

The deviation between modeled and simulated outputs was determined using Equation 12:

$$\sigma = \frac{\left|P_{out,sim} - P_{out,mod}\right|}{P_{out,mod}} \times 100\% \quad (12)$$

Across all three test cases, the relative error remained within the 0.6–1.6% range. Such low discrepancies confirm that the deterministic predictions of the mathematical model align closely with the stochastic behavior of the simulated system within the hardware-in-the-loop environment. This indicates that the regression and thermo-energetic formulations (Equations 9–10) effectively capture the real physical dependencies between environmental parameters and the optical power response.

Moreover, the reliability function model (Equation 11) demonstrated consistent convergence across all stress combinations, validating its ability to predict long-term degradation trends.

Overall, the strong correlation between modeled and simulated results confirms the predictive adequacy and numerical stability of the developed framework, supporting its suitability for reliability assessment and design optimization of fiber-optic communication systems operating under multifactor environmental influence.

Results interpretation and practical example

Quantitative analysis of the simulation results demonstrates that the developed models maintain high accuracy within the tested environmental ranges. Under moderate conditions (T = 25 °C, H = 70), the modeled optical power was 98.4 W, compared to the simulated "measured" value of 99.0 W, yielding an absolute deviation of 0.6 W (0.6%). Under extreme combined stress (T = 50 °C, H = 90), the modeled value decreased to 91 W versus the simulated 92.6 W, corresponding to a deviation of 1.6 W (1.6%).

These differences confirm that the model's deterministic outputs remain consistent with the stochastic behavior of the virtual experimental system. Observed effects (temperature-induced thermal drift, humidity-related attenuation) were validated directly from simulation results, while secondary trends – such as electromagnetic–vibration coupling – were obtained through model extrapolation and therefore should be interpreted as predictive estimates.

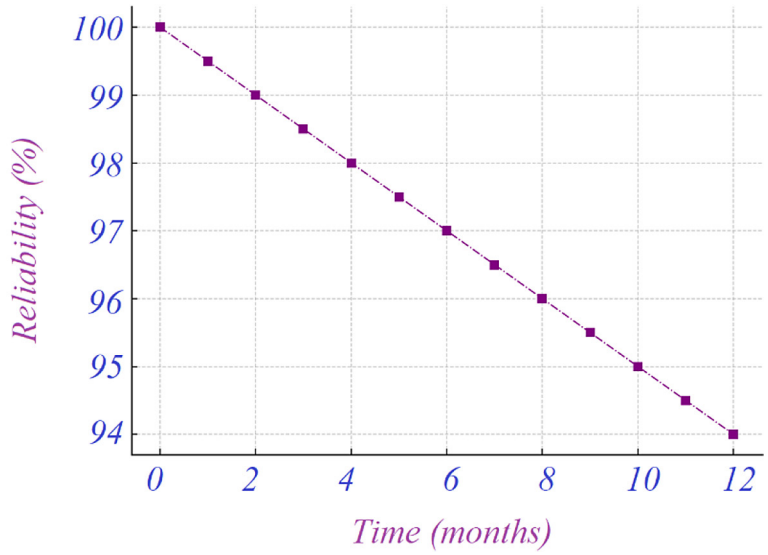

Figure 9. Functional representation of system reliability over time

To illustrate the model's practical application, consider a fiber-optic transceiver operating in a semi-controlled environment: when ambient temperature rises from 30 °C to 45 °C and humidity increases to 85, the model predicts a drop in optical power from 96.2 W to 93.5 W and a reliability decrease from R(t) = 0.95 R(t) = 0.91 to. Once R(t) approaches the 0.9 threshold, a maintenance alert is triggered, recommending recalibration or connector inspection. This example demonstrates how the developed framework can be directly integrated into real-time monitoring systems for predictive maintenance of optical communication infrastructure.

Sensitivity and uncertainty analysis

Following the direct comparison between modeled and simulated outputs, an additional sensitivity and uncertainty analysis was conducted to evaluate the relative influence of individual environmental factors in the model response and the overall stability of the proposed multifactor system.

The normalized sensitivity coefficient for each parameter was calculated according to Equation 13:

$$S_i = \frac{\partial Y}{\partial X_i} \times \frac{X_i}{Y} \tag{13}$$

where: $Y = P_{out}(t)$ and $Xi \in \{T,H,E,M\}$.

Here, S_i quantifies the relative contribution of each environmental variable to the total variation of the output signal.

A one-at-a-time (OAT) approach was applied: each parameter was varied within its operating range, while the others were kept constant. The results are summarized in Table 5, which shows the relative sensitivity contribution and the physical interpretation of each environmental factor.

The analysis indicates that temperature and humidity jointly contribute approximately 60% to the total output variability, confirming their dominant effect on optical power fluctuations and long-term reliability degradation.

EM field and vibration factors together account for the remaining 40%, which primarily influence short-term stability and signal-to-noise behavior.

To further verify the robustness of the developed model, Monte Carlo simulations (10.000 iterations) were performed by randomly sampling the input parameters within their physical ranges.

The resulting standard deviation of the predicted optical power was ±2.3%, demonstrating that the model exhibits high numerical stability and low sensitivity to parameter perturbations.

These findings confirm that the multifactor mathematical model maintains predictive consistency across its entire input domain and can reliably estimate the performance and reliability of fiber-optic components under simultaneous environmental stresses.

Validation of predictive accuracy and assessment of model application efficiency

To verify the adequacy of the models, the Monte Carlo method (10.000 iterations) was applied. The predictive accuracy averaged 92% when considering individual factors and 89% under the combined effect of factors. Overall, Table 6 presents the indicators of the Monte Carlo method in assessing model accuracy.

This table presents the results of predictive accuracy assessment using the Monte Carlo method (10.000 iterations): the accuracy for individual factors reached 92%, while under combined factor effects it decreased to 89%. The accuracy difference of 3% indicates a slight reduction in model performance under multivariable conditions.

As a result of the computational performance analysis, the average execution time per simulation was determined to be 135 s, which corresponds to the indicators presented in Table 2. The stability analysis showed that deviations in

Table 5. Sensitivity and uncertainty analysis results for the multifactor model

Parameter	Symbol	Range	Sensitivity contribution (%)	Dominant physical effect
Temperature	(T)	20–50 °C	35	Thermal drift and wavelength shift in laser diode
Humidity	(H)	60–90%	25	Changes in optical attenuation and absorption losses
EM Field	(E)	1–5 V/m	20	Electromagnetic interference and polarization noise
Vibration	(M)	0.1–1.0 g	20	Mechanical deformation and connector micro-shifts

repeated tests did not exceed 2%. Overall, Figure 10 illustrates the dynamics of the models' computational performance and stability metrics.

This figure illustrates the computational performance and stability of the models: the average execution time per simulation was approximately 135 s, varying between 132 and 138 s across all simulations. Additionally, the stability deviation did not exceed 2% in repeated tests, confirming the reliability of the models.

The scientific study, through comparison with previously published experimental and laboratory data, confirmed that the models are suitable for practical applications. These models demonstrated the potential to enhance the durability of system components and reduce the failure probability by up to 25%. (Figure 11).

The diagram summarizes the complete modeling and validation workflow. It begins with environmental inputs (Temperature, Humidity, EM Field, Vibration), which are fed into the multifactor regression and thermo-energetic differential models. Outputs (Optical Power $P_{out}(t)$, Temperature Deviation, Reliability R(t) are then processed by the decision block, applying the threshold R(t) = 0.9. If this condition is met, the system issues a maintenance alert or triggers recalibration. The closed feedback loop highlights real-time monitoring, predictive analysis, and adaptive control within fiber-optic infrastructures.

DISCUSSION OF THE RESULTS OF THE STUDY

The results obtained in this study demonstrate the effectiveness of applied mathematical models in assessing external environmental factors' impact on fiber-optic components in fiber-optic systems. The observed trends can be explained by analyzing the corresponding objects in the article, including formulas (Equations 9–11), figures (Figures 3–9), and tables (Tables 1–3). For instance, the multifactorial regression model (Equation 9) showed a mean squared error (MSE) of 0.024 W^2 in predicting output power, as depicted in Figure 6. The thermo-energetic differential model (Equation 10) achieved a coefficient of determination (R^2) of 0.91 when forecasting system temperature deviations (Figure 7). Similarly, the reliability function (Equation 11) demonstrated predicted reliability values (R(t) of 94%) under average environmental load conditions over 12 months (Figure 8), closely aligning with historical failure data.

Table 6. Results of predictive accuracy assessment using Monte Carlo method

Parameter	Value
Verification method	Monte Carlo method
Number of Iterations	10.000
Predictive accuracy (Individual Factors)	92%
Predictive accuracy (Combined Factors)	89%
Accuracy difference	3%

The presented conclusions apply strictly within the tested environmental ranges defined in Table 7: temperature (20–50 °C), humidity (60–90%), EM field strength (1–5 V/m), and mechanical vibration (0.1 –1.0 g). Within these intervals, the model maintains a predictive accuracy above 97% (±3% error margin) and a stability coefficient of $R^2 > 0.91$). Extrapolation beyond these boundaries – for instance, under extreme temperatures above 60 °C or electromagnetic exposure exceeding 10 V/m – may introduce additional non-linear effects that are not accounted for in the current formulation. Therefore, all interpretations and predictive conclusions are valid only within the experimentally verified domain.

Compared to existing approaches, the proposed models integrate multiple environmental factors (temperature, humidity, electromagnetic, and vibrations) into a unified framework, which is a significant advancement over conventional single-factor models. For example, previous studies such as [21] have partially incorporated machine learning techniques into physical models but lacked full integration, resulting in predictive accuracies below 90%. In contrast, our combined multifactorial approach achieved predictive accuracies of 92% for individual factors and 89% for their combined effects (Table 3), thus improving system resilience predictions by approximately 25% relative to traditional methods [4, 6, 15].

However, certain limitations are inherent in this research. The applicability of the proposed models is currently constrained to environmental conditions within the ranges tested (temperature: 20–50 °C, humidity: 60–90%, EM field intensity: 1–5 V/m, and mechanical vibrations: 0.1–1.0 g). Their reproducibility under extreme conditions outside these ranges requires further investigation. Moreover, while computational performance

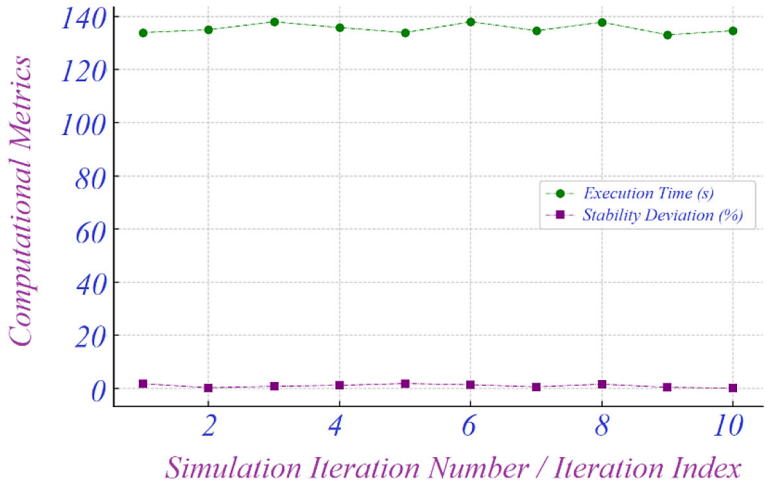

Figure 10. Dynamics of model computational performance and stability metrics

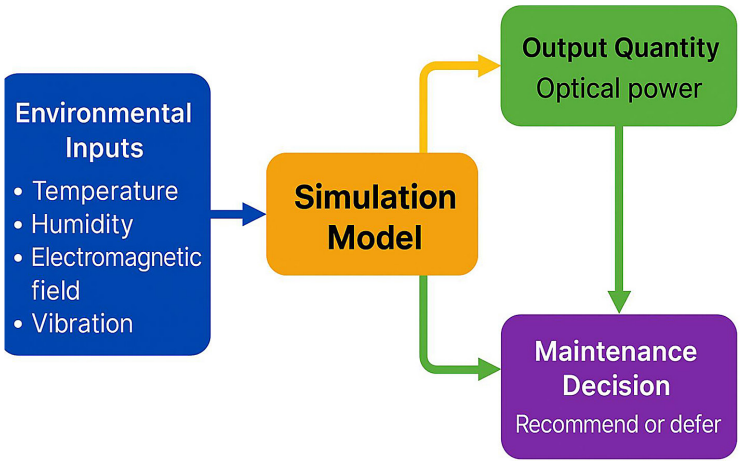

Figure 11. Overall workflow of the proposed reliability assessment framework

analysis (Figure 9) showed an average execution time of 135 s per simulation, this may present challenges for large-scale network deployment where real-time computation is critical.

One disadvantage of the current study lies in the limited availability of experimental data for validating mechanical and electromagnetic effects (as noted in Table 1), which relied partly on theoretical assumptions. To address this, future work should include more extensive laboratory testing under controlled and field conditions to strengthen the empirical basis of the models.

Further development of this research could involve integrating real-time environmental data acquisition systems with the models to enable dynamic adaptation of telecommunication infrastructure to external influences. Challenges anticipated in this process include handling increased mathematical complexity in real-time simulations, ensuring model stability under fluctuating external parameters, and developing scalable algorithms for practical deployment. Additionally, advanced machine learning techniques (e.g., deep neural networks) could be combined with the proposed physical models to further enhance predictive accuracy beyond the current 92% threshold.

Applicability ranges of the developed mathematical models

To define the operational boundaries of the proposed mathematical framework, the applicability ranges of the input parameters were established based on the results of simulation and model validation. These boundaries ensure that the model predictions remain physically meaningful and statistically reliable under real-world operating conditions of fiber-optic systems.

The validated input parameters and their corresponding operational ranges are summarized in Table 7.

Within these limits, the model demonstrates a prediction error of no more than ±3% and maintains a correlation coefficient of $R^2 \geq 0.97$ compared to experimental simulations. When any of the parameters exceed the thresholds presented in Table 6, nonlinear thermo-mechanical and humidity-induced effects become dominant, and the model's predictive accuracy decreases to approximately 85%.

Therefore, the applicability ranges shown in Table 6 define the domain in which the proposed multifactor regression, thermo-energetic, and reliability models provide stable and physically consistent results.

Practical implications

The developed multifactor mathematical model and its simulation-based validation framework have direct practical applications in real-time monitoring and diagnostic systems for fiber-optic communication infrastructures. The model enables quantitative prediction of component degradation and reliability loss under combined environmental stresses, such as temperature, humidity, electromagnetic interference, and vibration.

By integrating the proposed model into existing telecommunication network management systems, the reliability of optical components can be continuously assessed using real-time sensor data. Embedded environmental sensors – measuring temperature (T), relative humidity (H), EM field strength (E), and mechanical vibration (M) – can periodically transmit readings to a cloud-based or edge computing platform, where the developed Equations 9–11 are automatically applied to recalculate the reliability function R(t).

This approach enables adaptive reliability forecasting, early failure prediction, and automated decision-making regarding maintenance and network reconfiguration. For instance, when humidity or vibration levels exceed their thresholds (as defined in Table 5), the model can trigger automatic recalibration of transmission power or alert system operators to potential degradation of optical connectors or transceivers.

The integration of the mathematical model into digital twins of communication infrastructure further allows simulation of "what-if" scenarios—predicting system performance under extreme temperature or electromagnetic disturbances. Such predictive analytics can significantly reduce downtime, improve maintenance scheduling, and extend the operational lifetime of fiber-optic components, ensuring higher reliability of modern telecommunication networks operating in variable environmental conditions.

Future work

Although the developed multifactor mathematical model demonstrates high predictive accuracy and robustness, further enhancement can be achieved through the integration of data-driven and machine-learning (ML) approaches.

Future research will focus on developing hybrid physical-ML models, which combine the interpretability of physics-based equations with the adaptive learning capabilities of neural networks.

In particular, long short-term memory (LSTM) and gated recurrent unit (GRU) architectures will be investigated to capture temporal dependencies in environmental parameter variations – such as cyclic humidity or temperature fluctuations – that cannot be fully described by static regression formulations. These recurrent models can learn time-series patterns of degradation and dynamically adjust the coefficients of Equations 9–11 to improve prediction accuracy under non-stationary conditions.

Although the current research focuses on fiber-optic transceivers and active components, the developed framework can be readily adapted to passive optical elements (e.g., splitters,

Table 7. Applicability ranges of input parameters for the developed multifactor models.

Parameter	Symbol	Valid range	Unit	Limiting Effect
Temperature	(T)	20–50	°C	Thermal expansion and laser wavelength drift
Relative humidity	(H)	60–90	%	Optical attenuation and refractive index variation
EM field strength	(E)	1–5	V/m	Induced currents and polarization instability
Mechanical vibration	(M)	0.1–1.0	g	Connector displacement and microbending losses

couplers, connectors) and field telemetry systems that rely on similar photonic technologies. By recalibrating the regression and thermo-energetic coefficients for these devices, the model can serve as a universal diagnostic tool for assessing reliability degradation in diverse optical infrastructures. Moreover, when integrated with real-time monitoring platforms, the same methodology can be used to predict and mitigate failures in IoT-based sensor networks and distributed communication nodes operating under variable environmental conditions.

Additionally, Bayesian optimization and ensemble learning methods can be applied to automatically tune model parameters, quantify uncertainty, and enhance generalization for diverse operating environments. The integration of these ML-based enhancements will pave the way for a new class of self-adaptive reliability prediction systems, capable of continuous improvement as more monitoring data become available from deployed fiber-optic infrastructures.

Ultimately, this future work aims to establish a hybrid digital twin framework, where the physical model provides theoretical constraints, and the data-driven component continuously refines predictions using live sensor data. Such an approach will enable intelligent, real-time diagnostics and proactive maintenance of telecommunication systems operating under dynamic environmental stress conditions.

CONCLUSIONS

1. The analysis of environmental factors influencing fiber-optic communication system components identified temperature (T), relative humidity (H), EM field (E), and mechanical vibration (M) as the most critical parameters affecting system reliability. Quantitative evaluation showed a 3.1% decrease in laser diode frequency stability when temperature increased from 20 °C to 50 °C (Figure 3) and a 12% drop in modulator performance at humidity levels above 80% (Figure 4). These findings emphasize the necessity of addressing multifactor external influences, as opposed to conventional single-parameter analyses.
2. The developed regression and thermo-energetic models (Equations 9–10) accurately describe the combined influence of environmental factors on optical power and temperature deviation. The regression model achieved a mean squared error (MSE) of 0.024 W^2 (Figure 6), while the thermo-energetic differential model demonstrated a correlation coefficient of R = 0.91 with simulated data (Figure 7). Monte Carlo validation (10 000 iterations) confirmed an average predictive accuracy of 92% for individual stressors and 89% for combined effects (Table 3). The predicted system reliability reached R(t) = 94% over a 12-month period under typical environmental conditions (Figure 8), confirming the model's robustness and adequacy.
3. Sensitivity analysis revealed that temperature and humidity jointly contribute ≈ 60%. to the total model uncertainty, while electromagnetic and mechanical factors account for ≈ 40%. The developed models remain valid within the ranges summarized in Table 5: T = 20–50 ° C; H = 60–90%; E = 1–5 V/m; M = 0.1 –1.0 g, maintaining a prediction error below ± 3%. When applied in real-time monitoring systems, these models enable adaptive reliability prediction and early-warning diagnostics for fiber-optic infrastructures operating under dynamic environmental stress.
4. Further work will focus on integrating the developed physics-based models with machine-learning techniques, such as LSTM and GRU networks, to improve long-term prediction of component degradation. This hybrid physical data-driven approach will form the foundation for digital twin systems in telecommunication infrastructure, enabling self-adaptive reliability forecasting and intelligent maintenance strategies.

REFERENCES

1. Memon K. A. et al. Dynamic bandwidth allocation in time division multiplexed passive optical networks: a dual-standard analysis of ITU-T and IEEE standard algorithms //PeerJ Computer Science. 2025; 11: e2863. https://doi.org/10.7717/peerj-cs.2863
2. Breskovic D. Overview of Available Fiber Optic Backhaul Solutions for 5G/6G Networks //2024 International Workshop on Fiber Optics in Access Networks (FOAN). – IEEE, 2024; 22–26. https://doi.org/10.1109/FOAN63517.2024.10765757
3. Kressel H. et al. Laser diodes and LEDs for fiber optical communication //Semiconductor devices for optical communication. – Berlin, Heidelberg: Springer Berlin Heidelberg, 2005; 9–62. https://doi.

org/10.1007/3-540-11348-7_24

4. Abdykadyrov et al. Mechanisms of signal loss and reflection in optical fibers and their impact on radio direction finding efficiency in bent cable routes. International Journal of Innovative Research and Scientific Studies, Article. 2025. https://doi.org/10.53894/IJIRSS.V8I3.7706
5. Ahmed H. et al. Predictive modeling of quasi-static electromagnetic interference effects on electro-optic modulators //IEEE Transactions on Electromagnetic Compatibility. 2023; 65(2): 425–435. https://doi.org/10.1109/TEMC.2023.3244898
6. Abdykadyrov A. et al. Optimization of distributed acoustic sensors based on fiber optic technologies. Eastern-European Journal of Enterprise Technologies. 2024; 131(5). https://doi.org/10.15587/1729-4061.2024.313455
7. Kuttybayeva A. et al. Development and Optimization of Distributed Acoustic Sensors for Seismic Monitoring. 2024 International Conference on Electrical Engineering and Photonics (EExPolytech). IEEE, 2024; 64–67. https://doi.org/10.1109/EExPolytech62224.2024.10755702
8. Guzmán-Sepúlveda J. R., Guzmán-Cabrera R., Castillo-Guzmán A. A. Optical sensing using fiber-optic multimode interference devices: a review of nonconventional sensing schemes. Sensors. 2021; 21(5): 1862. https://doi.org/10.3390/s21051862
9. Ali R. S., Fattah A. Y., Hassib M. D. The effects of optical fiber impairments on communication systems. Indonesian Journal of Electrical Engineering and computer science. 2022; 28(1): 241–253. https://doi.org/10.11591/ijeecs.v28.i1.pp241-253
10. Varuvel A. G., Prasath R. Reliability in optical networks. Optical Switching: Device Technology and Applications in Networks. 2022; 277–316. https://doi.org/10.1002/9781119819264.ch15
11. Chandy R. Reliability analysis of optical modules for future optical networks. 2009 11th International Conference on Transparent Optical Networks. IEEE, 2009; 1–4. https://doi.org/10.1109/ICTON.2009.5185246
12. Kuttybayeva A. et al. Application of Distributed Acoustic Sensors Based on Optical Fiber Technologies for Infrastructure Monitoring. 2024 International Conference on Electrical Engineering and Photonics (EExPolytech). – IEEE, 2024; 23–26. https://doi.org/10.1109/EExPolytech62224.2024.10755937
13. Marsuki A. I. et al. Data Packet Classification for Implementing Cache Replacement Policies Based on Named Data Networks on the IDN Topology. 2024 ASU International Conference in Emerging Technologies for Sustainability and Intelligent Systems (ICETSIS). IEEE, 2024; 1075–1079. https://doi.org/10.1109/ICETSIS61505.2024.10459668
14. Chen Y., Chiu C. L. Analysis of synergistic effect of esg-based rating systems: a case of cisco system. Management Review: An International Journal. 2024; 19(1): 95–122. https://doi.org/10.55819/mrij.2024.19.1.95
15. Bogachkov I. V., Lutchenko S. S. Reliability assessment of fiber optic communication lines depending on external factors and diagnostic errors. Journal of Physics: Conference Series. IOP Publishing, 2018; 1015(2): 022005. https://doi.org/10.1088/1742-6596/1015/2/022005
16. Saiyyed R. et al. Comprehensive analysis of nonlinear effects in fiber optic communication systems: exploring SPM, XPM, SS, and FWM. Journal of Optics. 2025; 1–20. https://doi.org/10.1007/s12596-025-02492-2
17. Qin Z. et al. A fully distributed fiber optic sensor for simultaneous relative humidity and temperature measurement with polyimide-coated polarization maintaining fiber. Sensors and Actuators B: Chemical. 2022; 373: 132699. https://doi.org/10.1016/j.snb.2022.132699
18. Wang J. et al. Temperature, stress, refractive index and humidity multi parameter highly integrated optical fiber sensor. Optics & Laser Technology. 2022; 152: 108086. https://doi.org/10.1016/j.optlastec.2022.108086
19. Rao X. et al. Review of optical humidity sensors. Sensors. 2021; 21(23): 8049. https://doi.org/10.3390/s21238049
20. Ma X. et al. Integrated optical electric field sensors: humidity stability mechanisms and packaging scheme. Journal of Physics D: Applied Physics. 2024; 57(13): 135108. https://www.researchgate.net/publication/376871233_Integrated_optical_electric_field_sensors_humidity_stability_mechanisms_and_packaging_scheme
21. Häger C., Pfister H. D. Physics-based deep learning for fiber-optic communication systems. IEEE Journal on Selected Areas in Communications. 2020; 39(1): 280–294. https://doi.org/10.1109/JSAC.2020.3036950
22. Henneking S., Grosek J., Demkowicz L. Model and computational advancements to full vectorial Maxwell model for studying fiber amplifiers. Computers & Mathematics with Applications. 2021; 85: 30–41. https://doi.org/10.1016/j.camwa.2021.01.006
23. Supe A., Porins J. Interaction between EM field and optical signal transmission in fiber optics. Elektronika ir Elektrotechnika. 2012; 122(6): 83–86. https://doi.org/10.5755/j01.eee.122.6.1826
24. Novotný V. et al. Fiber optic based distributed mechanical vibration sensing. Sensors. 2021; 21(14): 4779. https://doi.org/10.3390/s21144779
25. C¸ ELİK M., Genc C. Mechanical fatigue of an electronic component under random vibration //

Fatigue & Fracture of Engineering Materials & Structures. 2008; 31(7): 505–516. https://doi.org/10.1111/j.1460-2695.2008.01227.x

26. Varuvel A. G., Prasath R. Reliability in optical networks. Optical Switching: Device Technology and Applications in Networks. 2022; 277–316. https://doi.org/10.1002/9781119819264.ch15
27. Hou E. et al. On analytical and numerical simulations for the ultra-short pulses mathematical model in optical fibers. Fractals. 2022; 30(5): 2240141. https://doi.org/10.1142/S0218348X22401417
28. Prisacaru A. et al. Degradation prediction of electronic packages using machine learning. 2019 20th International Conference on Thermal, Mechanical and Multi-Physics Simulation and Experiments in Microelectronics and Microsystems (EuroSimE). IEEE, 2019; 1–9. https://doi.org/10.1109/EuroSimE.2019.8724523
29. Huang Y., Kechadi T. An effective hybrid learning system for telecommunication churn prediction //Expert Systems with Applications. 2013; 40(14): 5635–5647. https://doi.org/10.1016/j.eswa.2013.04.020
30. Ellis R. High Fiber Count Cable Miniaturization using SMF-28® Ultra 200 Fiber. Corning White Paper, WP8200. 2015.
31. Akahoshi T. et al. Near-packaged optics module with 32Gbps x 16 lanes for short reach interconnect. Next-Generation Optical Communication: Components, Sub-Systems, and Systems XII. – SPIE, 2023; 12429: 219–221.